



Pergamon

Mapping the Kinase Domain of Janus Kinase 3

Christopher Adams, David J. Aldous,* Shelley Amendola, Paul Bamborough, Colin Bright, Sarah Crowe, Paul Eastwood, Garry Fenton, Martyn Foster, Trevor K. P. Harrison, Sue King, Justine Lai, Christopher Lawrence, Jean-Philippe Letaliec, Clive McCarthy, Neil Moorcroft, Kenneth Page, Sudha Rao, Jane Redford, Shazia Sadiq, Keith Smith, John E. Souness, Sukanthini Thurairatnam, Mark Vine and Barry Wyman

Aventis Pharmaceuticals, 1041 Route 202–206, PO Box 6800, Bridgewater, NJ 08807, USA

Received 24 April 2003; accepted 22 May 2003

Abstract—The utilization and impact of parallel synthesis on lead exploration around initial hit oxindole (**1**) are described. The emergent SAR, analogue design and functional impact will also be detailed.

© 2003 Published by Elsevier Ltd.

There has been intensive effort to discover and exploit selective kinase inhibitors.^{1,2} The ubiquitous nature of kinases, coupled to the high homology in the ATP binding domain, have presented medicinal chemists with a myriad of difficulties in advancing inhibitors for therapeutic evaluation.

We became interested in Janus Kinase 3 (JAK 3) protein tyrosine kinase, as a potential immune modulating target due to the functional impact of down-regulated JAK 3 signal in an immune compromised patient sub-population.^{3–5} The sub-population of the severe compromised immune deficient (SCID) and X-linked severe compromised immune deficient (X-SCID) patient pool displayed abnormal function in the JAK 3 signaling pathway either due to a mutation of the γ_c allele which mutated the γ_c chain so JAK 3 did not bind or a mutation directly impacting JAK 3.

Whilst the SCID and X-SCID patients were immune compromised we postulated that in auto-immune diseases where the immune system was up-regulated such as arthritis or diabetes modulation of JAK 3 might be an effective therapy.^{6–9}

In order to explore the therapeutic hypothesis, we embarked upon a focused screening. A clone of the kinase domain¹⁰ was generated and a HTRF assay formatted.¹¹ The initial screen of the kinase biased set yielded oxindole **1** as a μ M hit (Fig. 1).

To further refine the inhibitor, a homology model was generated. The model used as a template the complex between cyclic adenosine monophosphate (cAMP) dependent protein kinase (cAPK).¹² cAPK was chosen because at that time it was the only protein kinase whose structure had been solved in its active, or closed,¹³ conformation. The overall sequence identity between cAPK and human JAK3 (hJAK3) over the 256 aligned positions in the catalytic domain is 26%. Some time later, the insulin receptor tyrosine kinase (IRK), that shares 32% sequence identity with JAK3, was crystallized in an active conformation¹⁴ with an ATP analogue, adenylyl imido-diphosphate (AMP-PNP). A

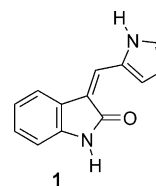


Figure 1. Initial oxindole.

*Corresponding author. E-mail: david.aldous@aventis.com

second hJAK3 model was constructed using this as a template. The main differences between the two models arise from the more open pocket in the IRK-based model. Although IRK is more closely related to hJAK3 than is cAPK overall, when only the 29 residues closer than 5.5 Å from the AMP-PNP in the IIR3 structure are considered, 17 (59%) in IRK are identical to their aligned positions in hJAK3, compared to 19 (66%) in cAPK. The cAPK-based model was used to carry out most of this work and that is referred to in the text.

In JAK 3, ATP and the oxindole inhibitor were predicted to donate a hydrogen bond to the backbone carbonyl of residue Glu903 and to accept a hydrogen bond from the backbone NH of Leu 905 (Fig. 2).

The oxindole **1** was docked into the modeled protein active site, initially by fitting the acceptor–donor pair of **1** onto the acceptor–donor pair of ATP. As observed in the Fibroblast Growth Factor (FGF) Receptor complex,¹⁵ the double bond was modeled in the *Z*-isomer configuration. The *Z*-isomer is the dominant configuration due to an internal hydrogen bond between the oxindole oxygen and the pyrrole NH.¹⁶ When docked, the oxindole core sits in the space between the two kinase lobes, making contact with Val 836, Ala 853, Val 884, Met 902 and Leu 905.

Analysis of the docked inhibitor indicated that the pyrrole ring projects outwards in the direction of solvent, and contacts Leu 956 and Gly 908. Although vectors leading away from the pyrrole ring at the 4'- and 5'-position point towards solvent, the ring itself lies within the ATP pocket. Variation at this region in the library was intended to explore this space fully, to identify possible interaction sites both inside the pocket and outside on the lip, but also to explore the potential for the attachment of groups to give better pharmacological properties without necessarily interacting with the kinase.

In contrast, before and after refinement, it could be seen that the vector of the CH atom at the 5-position of the oxindoles core pointed into an unfilled region of the active site. Crystal structures of complexes of CDK2–staurosporine¹⁷ and cAPK–staurosporine,¹⁸ as well as

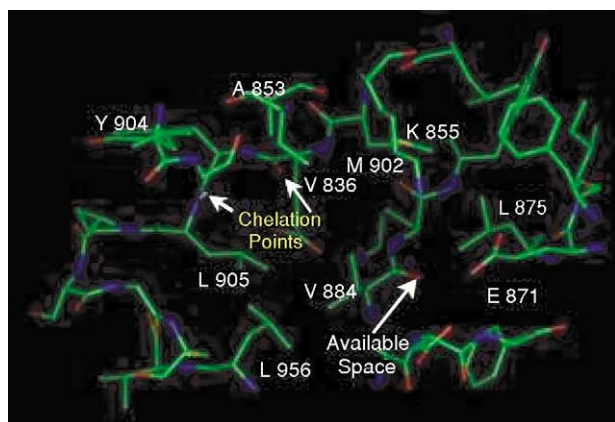


Figure 2. JAK 3 homology model.

of the SB203580–p38 kinase complex,¹⁹ have shown a hydrophobic part of the inhibitors projecting into a similar area at the rear of the ATP pocket. The hydrophobic residues Leu 875, Leu 900 and Met 902 lie around this region. However, acidic and basic side chains (Lys 855 and Glu 871) are also nearby. In many complexes of kinases with ATP, the conserved equivalent of Lys 855 binds to the ATP phosphates and forms a salt bridge with Glu 871.²⁰ A diverse set was defined to probe this region (Fig. 3).

We identified proprietary and commercially available aldehydes to deliver a two-dimensional array by condensation of oxindole cores (Scheme 1).

The product precipitated out resulting in >85% pure product.²¹ The final array consisted of 700 inhibitors which were then screened against the JAK 3 kinase domain.

We analyzed the impact of the substitution at the 5-position of the oxindole core keeping the pyrrole constant (Table 1).

Nitro afforded no improvement whilst the keto, acid and amide improved potency approximately 5-fold. However, reversing the amide reduced potency, implying that electron withdrawal was important which was reinforced further by the potent keto thiophene. Interestingly, the reduced hydroxy thiophene was potent, albeit an order of magnitude less than the keto analogue, implying a strong aryl interaction in this region. The 3-pyridyl reinforced the need for electron withdrawal with bulk at the 5-position.

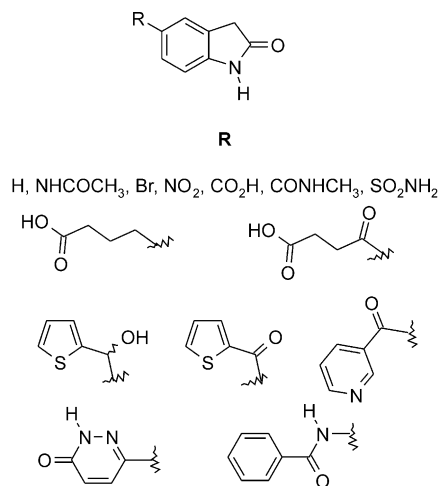
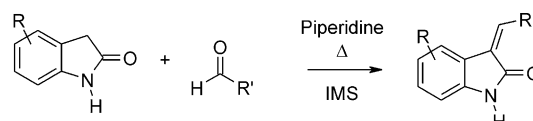
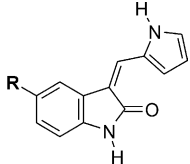
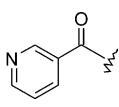
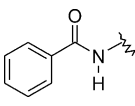
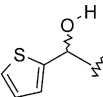
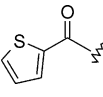


Figure 3. 5-Position probes.



Scheme 1. Condensation to target inhibitors (IMS, industrial methylated spirit).

Table 1. Selected 5-position substitution with pyrrole constant


Compd	5-Position substitution R	JAK 3 inhibition (IC ₅₀ , μM)
1	H	0.900
2	NO ₂	0.710
3		0.168
4	CO ₂ H	0.213
5		0.21
6		0.870
7		0.190
8		0.026
9		0.027

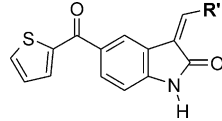
When the keto thiophene was constant, the impact of varying the aldehyde was defined (Table 2).

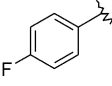
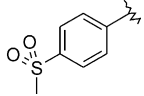
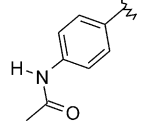
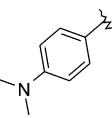
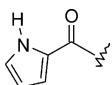
Electron-donating aromatics increased potency with the most potent being pyrrole.

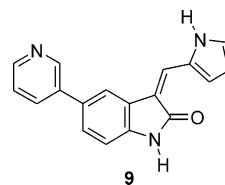
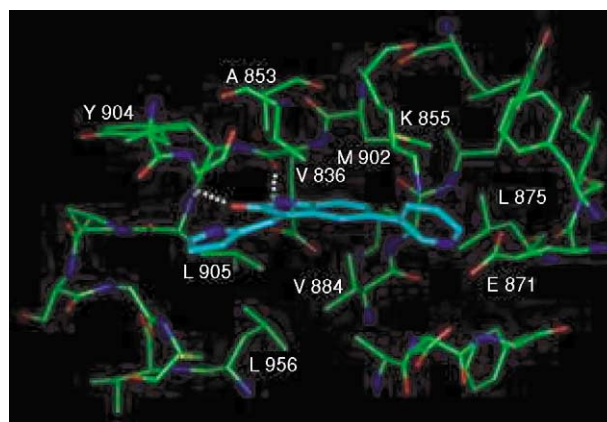
One of the most active compounds in the library, IC₅₀ 27 nM, had a 3'-pyridyl at the 5-position (Fig. 4).

The 3'-pyridyl inhibitor **9** was docked into the active site of JAK 3 (Fig. 5).

The pyridyl ring is positioned deep within the pocket, surrounded by Leu 875, Leu 900, Met 902 and the hydrophobic part of the Lys 855 side chain. Interestingly, this part of the crystal structure of FGF receptor complexed with SU5402 is occupied by a group of three water molecules, probably hydrogen-bonding to Lys-514 and Glu-531, which are the residues in the FGF receptor corresponding to Lys 855 and Glu 871 of JAK

Table 2. Selected aldehyde variation with keto thiophene constant


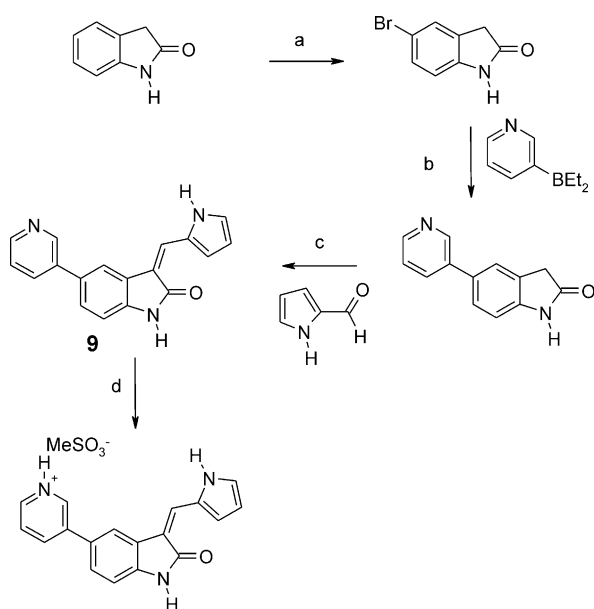
Compd	Aldehyde R'	JAK 3 inhibition (IC ₅₀ , μM)
10		2.3
11		4.9
12		7.1
13		0.70
14		0.20
15		0.26
8		0.026

**Figure 4.** 3'-Pyridyl oxindole inhibitor.**Figure 5.** Docked 3'-pyridyl inhibitor **9**.

3. The burial of hydrophobic groups into this pocket and the consequent displacement of these waters probably accounts for the increased affinity of the 3'-pyridyl compared to the initial oxindole **1**.

Although the precipitation of the target analogue was a great asset in the rapid construction of the library, it highlighted solubility as a key property for analogue progression and inhibitor design. The free base of the 3'-pyridyl inhibitor **9** had a solubility in water of < 1 mg/L whilst the mesylate salt had a solubility of 3600 mg/L. The synthesis of the 3'-pyridyl inhibitor **9** is outlined in Scheme 2.

As the nascent SAR implied that electron withdrawing imparted superior potency we decided to explore the SAR further by the synthesis of aza oxindoles.^{22,23} The aza analogues introduced an electron deficient aryl along with an additional salt handle to enhance solubility (Table 3).



Scheme 2. Synthesis 3'-pyridyl oxindole: (a) KBr, Br₂/H₂O, 94%; (b) Pd(PPh₃)₄, THF, 30%; (c) EtOH/piperidine, 80%; (d) MeSO₃H, THF, 87%.

Table 3. Selected 5-aryl substitution with pyrrole constant

Compd	X, ¹ X, ² X	JAK 3 inhibition (IC ₅₀ , μM)
9	X, ¹ X, ² X = CH	0.027
16	X = N	0.235
17	¹ X, ² X = CH	0.030
18	¹ X = N X, ² X = CH	0.350
	² X = N X, ¹ X = CH	

The introduction of nitrogen at the 4-position, **16**, resulted in a 10-fold loss in potency. The drop off in potency for **16** can be rationalized by the introduction of conformational mobility (Fig. 6).

The NMR studies showed a single isomer to be present for analogues **9**, **17** and **18**. In the case of analogue **16**, a mixture of conformations was observed. Others have observed this conformational stability and mobility.¹⁶ We rationalized the drop off in potency for **18** as a distribution of the hydrogen bonding of the NH of the oxindole.

We designed a filtering cascade for progression of JAK 3 inhibitors that relied upon the inhibition of IL-2 induced proliferation on both mouse CTLL²⁴ cells and human T-cells. In addition, the analogues were required to inhibit JAK 3 and STAT 5 phosphorylation.²⁵

The basis for the filtering cascade stemmed from the understanding of the function of Janus kinases being cytoplasmic tyrosine kinases involved in signal transduction. Binding of IL-2 to its receptor triggers oligomerization of the receptor chain, which activates Janus kinases. Activated JAK 3 then autophosphorylates, phosphorylates a member of the STAT family, STAT 5

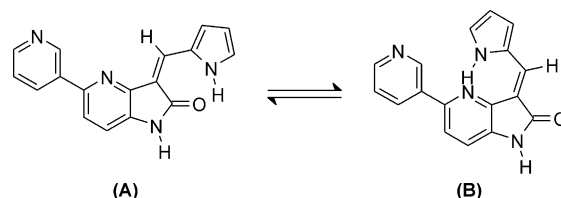


Figure 6. Conformational studies on aza oxindoles **16**.

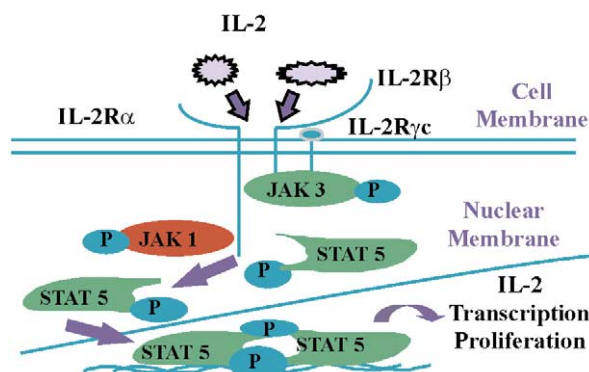


Figure 7. Signaling through the IL-2 receptor.

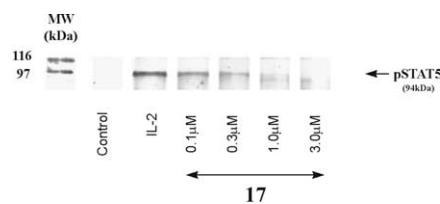


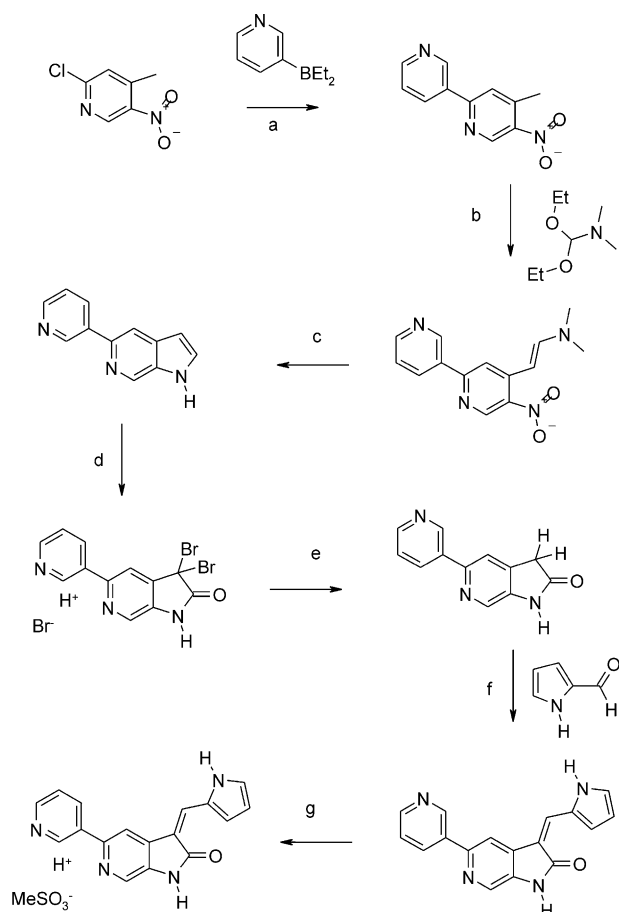
Figure 8. Anti-phosphotyrosine antibody probed Western blot showing concentration-dependent inhibition of IL-2 induced STAT 5 tyrosine phosphorylation by inhibitor **17** in CTLL cells.

on specific tyrosyl residues. Upon phosphorylation of specific, STAT proteins become activated and form homo or hetero dimeric complexes that translocate to the nucleus, bind to specific DNA sequences and alter the expression of cytokine regulated genes (Fig. 7).^{26,27}

Inhibitors **9** and **17** inhibited STAT 5 phosphorylation (Fig. 8), JAK 3 kinase activity and JAK 3 phosphorylation (Table 4) with similar potency. Inhibitor **17** exhibited an improved efficacy profile in the IL-2 proliferation assays, which we speculated might be due to differences in physical form. The inhibitors **9** and **17** were not profiled against mouse JAK 3i, therefore the compression in the mouse CTLL assay can only be speculated as being the result of orthologue differences. However,

Table 4. Whole cell profiling

Compd	> JAK 3 inhibition (IC ₅₀ , μM)	Inhibition of phosphorylation at 3 μM		Inhibition of IL-2 induced proliferation (IC ₅₀ , μM)	
		STAT 5	JAK 3	CTLL (mouse)	T-Cell (human)
9	0.027	Yes	Yes	0.76	0.25
16	0.235	No	Yes	0.92	0.70
17	0.030	Yes	Yes	0.45	0.03
18	0.350	No	—	2.3	2.0



Scheme 3. Synthesis 3'-pyridyl aza oxindoles **17**: (a) Pd(PPh₃)₄, THF/H₂O, NaHCO₃, Δ, 52%; (b) DMF, Δ, 52%; (c) H₂/Pd/C, IMS, 81%; (d) NBS, *t*BuOH, H₂O, 88%; (e) H₂/Pd/C, IMS, Et₃N, 36%; (f) EtOH/piperidine, Δ, 80%; (g) MeSO₃H, THF, 87%.

analogues **16** and **18** did not inhibit STAT 5 phosphorylation and had reduced efficacy in the IL-2 proliferation assays (Table 4). Neither analogue was progressed further.

The aza oxindole **17** was synthesized as outlined in Scheme 3.

Inhibitors **9** and **17** were profiled in cassette dosing PK studies which clearly demonstrated the enhancement in bioavailability due to the formation of the salt, Table 4 (Table 5).

Inhibitor **9** attenuated the increase in ear weight in the oxazolone-induced ear oedema model,²⁸ indicating an action upon the reactivation of the immune response and/or upon the inflammatory response, which is produced. The efficacy of **9** was comparable to that of the steroid dexamethasone (10 μg/ear) administered in acetone (Fig. 9).

In conclusion, we identified a weak inhibitor of JAK 3 which formed the basis for parallel synthesis to construct

Table 5. CombiPK data following ip administration at 1 mg/kg

Compd	Cp max (ng/mL)	T _{max} (h)	AUC _{0-∞} (h ng mL ⁻¹)	Terminal T _{1/2} (h)
9	600–1400 (< 50) ^a	0.5	7686 (< 500) ^a	3.0
17	700–1400	0.5	4579	3.3

^aFree base.

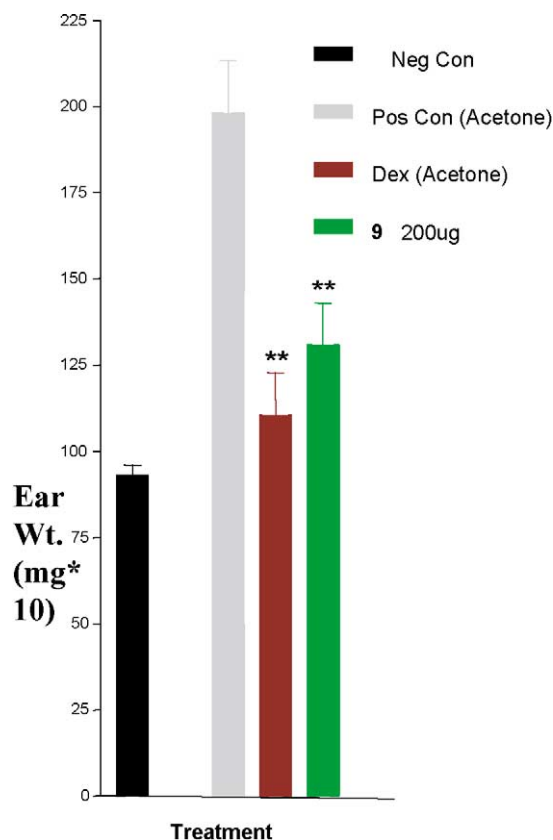


Figure 9. Oxazolone induced ear oedema in mouse.

a 700 component library. The library was designed based on the docking into the homology model of the hit **1**. Low-nM inhibitors emerged from the library that had a good correlation of JAK 3 inhibition linked to signal related functional impact. Finally, the inhibitor **9** demonstrated an effect comparable to dexamethasone in the ear odema model.

References and Notes

1. Sridhar, R.; Hanson-Painton, O.; Cooper, Denise, R. *Pharmaceut. Res.* **2000**, *17*, 1345.
2. Fabbro, D.; Parkinson, D.; Matter, A. *Curr. Opin. Pharmacol.* **2002**, *2*, 374.
3. Russell, S. M.; Johnston, J. A.; Noguchi, M.; Kawamura, M.; Bacon, C. M.; Friedmann, M.; Berg, M.; McVicar, D. W.; Witthuhn, B. A.; Silvennoinen, O. *Science* **1994**, *266*, 1042.
4. Noguchi, M.; Rosenblatt, H. M.; Filipovich, A. H.; Adelstein, S.; Modi, W. S.; McBride, O. W.; Leonard, W. J. *Cell* **1993**, *73*, 147.
5. Leonard, W. J. *Annu. Rev. Med.* **1996**, *47*, 229.
6. Leonard, W. J.; O'Shea, J. J. *Annu. Rev. Immunol.* **1998**, *16*, 293.
7. Sugamura, K.; Asao, H.; Kondo, M.; Tanaka, N.; Ishii, N.; Ohbo, K.; Nakamura, M.; Takeshita, T. *Annu. Rev. Immunol.* **1996**, *14*, 179.
8. Sudbeck, E.; Uckun, F. *IDrugs* **1999**, *2*, 1026.
9. Cetkovic-Cvrlje, M.; Dragt, A. L.; Vassilev, A.; Liu, X. P.; Uckun, F. M. *Clin. Immunol.* **2003**, *106*, 213.
10. The protein was expressed with an N-terminal FLAG tag using the in-house expression vector pYOUNG and the yeast strain *Kluveromyces lactis*. The recombinant protein was expressed intracellularly and was purified using M2 affinity resin.
11. **Homogenous time resolved fluorescence (HTRF) assay:** A selective synthetic tyrosine kinase containing substrate (biot-bA-bA-bA-L-P-L-D-K-D-Y-Y-V-V-R-E-P-G-Q[NH]₂) recognized by JAK3 (catalytic domain) is labeled with biotin. The substrate (1 μ M) is phosphorylated by JAK3 (50 ng/assay point) in the presence of ATP (8 μ M), DTT and Mg²⁺, 10 min at room temperature. APC-labeled streptavidin and a selected cryptate-labeled anti-phosphotyrosine are then added into the well in order to generate the specific signal that is proportional to the phosphorylated tyrosine concentration. After 1 h of incubation at room temperature, plates are read and the % δ_{\max} is determined using Packard discovery counter. The final DMSO concentration in the assay was 8%. The standard for the assay was oxindole **1**.
12. Zheng, J.; Trafny, E. A.; Knighton, D. R.; Xuong, N.-H.; Taylor, S. S.; Ten Eyck, L. F.; Sowadsky, J. M. *Acta Crystallogr.* **1993**, *D49*, 362.
13. Zheng, J.; Knighton, D. R.; Xuong, N.-H.; Taylor, S. S.; Sowadski, J. M.; Ten Eyck, L. F. *Protein Sci.* **1993**, *2*, 1559.
14. Hubbard, S. R. *EMBO J.* **1997**, *16*, 5572.
15. Mohammadi, M.; McMahon, G.; Sun, L.; Tang, C.; Hirth, P.; Yeh, B. K.; Hubbard, S. R.; Schlessinger, J. *Science* **1997**, *276*, 955.
16. Sun, L.; Tran, N.; Tang, F.; App, H.; Hirth, P.; McMahon, G.; Tang, C. *J. Med. Chem.* **1998**, *41*, 2588.
17. Lawrie, M. A.; Noble, E. M.; Tunnah, P.; Brown, N. R.; Johnson, L. N.; Endicott, J. A. *Nat. Struct. Biol.* **1997**, *4*, 796.
18. Prade, L.; Engh, R. A.; Girod, A.; Kinzel, V.; Huber, R.; Bossemeyer, D. *Structure* **1997**, *4*, 1627.
19. Tong, L.; Pav, S.; White, D. M.; Rogers, S.; Crane, K. M.; Cywin, C. L.; Brown, M. L.; Pargellis, C. A. *Nat. Struct. Biol.* **1997**, *4*, 311.
20. Johnson, L. N.; Noble, M. E.; Owen, D. J. *Cell* **1996**, *85*, 149.
21. 85% by LC/MS, was set as the lower limit for acceptance of each library component.
22. Robinson, R. P.; Donahue, K. M.; Son, P. S.; Wagy, S. D. *J. Heterocycl. Chem.* **1996**, *33*, 287.
23. Daisley, R. W.; Hanbali, J. R. *Synth. Commun.* **1981**, *11*, 743.
24. **IL-2 induced murine CTLL cell proliferation:** Seed CTLL's (2 \times 10⁴ cells/well) in 96-well plate, in the absence of IL-2, for 6 h. Add 10 U/mL recombinant human IL-2 at time zero. Add JAK 3 inhibitors in DMSO (final concentration 0.5%) at time zero. Add 1 μ Ci/well [³H]-thymidine at 18 h of culture. Harvest cells after 24 h, on to filter plates, and count scintillations [³H]-thymidine incorporation into DNA reflects extent of proliferation.
25. **IL-2 induced JAK 3 and STAT5 tyrosine phosphorylation:** Pretreat CTLL cells with JAK 3 inhibitors for 4 h. Stimulate cells with 10 U/mL IL-2 for 20 min, lyse cells and immunoprecipitate with anti-mouse JAK 3 and STAT5 antibodies. Subject immunoprecipitated samples to SDS-PAGE electrophoresis. Probe electrophoresized blots with anti-phosphotyrosine antibody.
26. Miyazaki, T.; Kawahara, A.; Fujii, H.; Nakagawa, Y.; Minami, Y.; Liu, Z. J.; Oishi, I.; Silvennoinen, O.; Witthuhn, B. A.; Ihle, J. N. *Science* **1994**, *266*, 1045.
27. Johnston, J. A.; Kamura, M.; Kirken, R. A.; Chen, Y. Q.; Blake, T. B.; Shibuya, K.; Ortalso, J. R.; McVicar, D. W.; O'Shea, J. J. *Nature* **1994**, *370*, 151.
28. **Protocol for oxazolone induced ear odema:** On day 1, female BALB/c mice were sensitized by topical application of oxazolone (100 μ L of 2% solution in acetone) to the shaved abdomen. On day 7, acetone (negative control group) or oxazolone (2% solution in acetone, remainder of animals) was applied topically to the right ear (10 μ L on each side of the ear). Test compounds or appropriate vehicles (acetone) were administered topically to the right ear (10 μ L on each side of the ear) 0.5 h after challenge. Mice were killed 24 h after challenge. A 6-mm disc of challenged (right) ear was removed and weighed.